Available online at www.sciencedirect.com

ScienceDirect

Procedia Manufacturing 00 (2019) 000–000

Procedia MANUFACTURING

www.elsevier.com/locate/procedia

18th International Conference Metal Forming 2020 Project

Manufacturing thin-walled 99.99% pure Zn tubes with ultrafine grained structures by flowforming

Magro T.[a,*], Ghiotti A.[a], Bruschi S.[a]

[a]*Università degli Studi di Padova, Department of Industrial Engineering, Via Venezia 1, 35121, Padova (IT)*

* Corresponding author. Tel.: +39 049 8276819. *E-mail address:* tommaso.magro.1@phd.unipd.it

Abstract

The last decade has seen several attempts to introduce bioresorbable prostheses in order to reduce the number of surgeries, but all the potentially interesting metallic alloys suffer of poor mechanical or chemical resistance. Zinc alloys are attracting more attention for producing temporary prosthesis devices thanks to their bioabsorbable characteristic in human environment, since they present a suitable corrosion resistance to human fluids. However, at the same time, they have extremely poor mechanical properties that make them still unsuitable for such applications. One possible way to increase mechanical performances is to refine the material grain using Severe Plastic Deformation (SPD) processes that can be traditionally used to obtain such refined microstructures through the application of high deformation rates under complex stress states. The paper focuses on the feasibility of using the backward tube flowforming process to obtain a significant grain refinement (below 1 µm) when applied to pure zinc alloy in order to increase its mechanical resistance to values suitable for load bearing temporary prostheses, starting from a 287 µm grain size material. A numerical FE simulation was adopted to understand the strain during the process while the influence of the process parameters, namely the reduction per pass, the mandrel speed and the feed rate, on the microstructural characteristics and related mechanical properties are shown and discussed.

Keywords: Zinc Alloy, Backward Tube Flowforming, Ultrafine Grain Material, Severe Plastic Deformation.

1. Introduction

Nowadays, metal prostheses are designed for permanent implantations (such as hips, dental prostheses, knees, etc.) or to supply just a temporary supporting function (e.g. fixing bone fractures). Although fundamental for a correct tissue healing, the latter require a second surgery, with negative effects for the patients' well-being and additional costs for the healthcare. Several attempts to introduce bioresorbable materials, such as magnesium or zinc, were made to manufacture bioabsorbable prostheses in order to decrease the number of surgeries, exploiting the mechanical properties for the former and the corrosion resistance to human fluids for the latter [1]. However, the poor chemical resistance for the magnesium alloy as well as the poor mechanical properties for the zinc alloys haven't allowed reliable design of bioabsorbable human prostheses using such materials.

The main limit appears being the grain size these alloys presents at room temperature, which governs the main physical, chemical, and mechanical properties and which is reliant on the process chain used to manufacture prosthetic implants. It is well known that the lower the grain size the higher the metal strength at room temperature, according to the Hall-Petch's relationship [2, 3], and that having a grain refinement until values between 100 and 1 µm could be extremely beneficial to obtain satisfactory mechanical properties as the ones requested for removable prosthetic applications. For this reason, it could be thought that infinitely reducing the grain size would significantly influence the mechanical properties, with positive effects for example on the

yield strength and ductility. However, in literature several researches reveal the impossibility of extrapolating the Hall-Petch relationship for grain sizes smaller than 1 μm. There is an ambiguity in the trend of the plot as the grain size falls down to a value below 25 nm: while some results predict a plateau, some others show an unexpected decrease [4].

Nomenclature

K	Yielding constant
σ_Y	Yield stress
σ_0	Friction stress
d	Grain size
L_0	Initial length of the tube
L_1	Final length of the tube
t_0	Initial thickness of the tube
t_1	Final thickness of the tube
E	Young modulus
d_{int}	Internal diameter
α	Roller forming angle
β	Roller sleeking angle
β’	Roller receding angle
l	Roller polishing belt length
r	Roller fillet radius

In anisotropic materials such as zinc and its alloys, characterized by a hexagonal close-packed (hcp) structure, higher strengths can be achieved by developing selected strong textures using the appropriate processing conditions. Severe Plastic Deformation techniques, hereafter SPD, have been utilized over the last two decades to refine the grain size of many materials, obtaining enhanced mechanical and physical properties. Several authors carried out SPD processes using titanium [5], aluminium [6] or magnesium [7] alloys, showing an increase in the mechanical properties, while, when using zinc alloys, the results were discordant and incomplete [1, 8, 9].

With focus on this uncovered aspect, the paper presents preliminary results of recent investigations carried out to assess the feasibility of an incremental backward flowforming process applied to a zinc tube, to explore the possibility of grain refinement that this class of manufacturing processes may allow, with consequent improvement of the mechanical properties for human prostheses applications. The first part describes the state of the art regarding the tube flowforming process, with details on the material and process parameters adopted in the experiments. Then a numerical finite element model of the backward tube flowforming process is presented, to compute the process forces and the strains as function of the main process parameters. In the final part of this paper the microstructures and the results of the microhardness tests that are carried out to evaluate the feasibility of the process are reported.

1.1. Severe Plastic Deformation processes

SPD is a generic term for a group of low-cost metal-machining techniques involving very large strain that provides the opportunity to achieve remarkable grain refinement in metals using different shapes of samples such as bulk, tube and sheet. The strain is imposed to the workpiece due to special tool geometries that prevent the free flow of the material and thereby produce significant hydrostatic compressive stresses. The presence of the hydrostatic pressure is a clue for reaching the high strains required for exceptional grain refinement and to prevent crack growth and other defects in the sample [5, 10]. The structural changes caused by SPD methods are reflected in improved mechanical properties, and the strength of all polycrystalline materials is related to the grain size, *d*, through the Hall-Petch equation, which states that the yield stress, σ_Y, is given by:

$$\sigma_Y = \sigma_0 + \frac{K}{\sqrt{d}} \quad (1)$$

where σ_0 is termed the friction stress and *K* is a yielding constant. The slope of the Hall-Petch line or *K* value for hcp metals is higher than that of body-centered cubic (bcc), and the *K* value of bcc is higher than that of face-centered cubic metals (fcc), as reported in Fig. 1. The figure shows small *K* value for fcc metals because of weakly locked dislocations and a multiplicity of slip system, and a small grain size dependence of the flow stress, large *K* value for hcp metals because of the limited slip systems, and relatively large *K* value for bcc metals because of the strong locking.

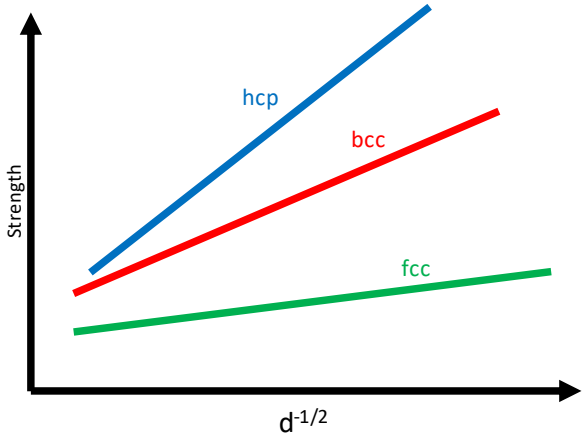

Fig. 1. The slope of the Hall-Patch line.

Various methods of SPD processes, developed over the last decades from conventional processes like extrusion, rolling and forging, can be used to produce bulk materials, sheets, and tubes and are characterized by the absence of mechanical defects, cracks, or porosity in the final parts. Extrusion has been frequently used to refine the grain size and make it homogeneous over the length and the cross-section. For instance, changing the direction of the material flow, as in the Equal Channel Angular Press (ECAP) [9, 11], applying cyclic loads and deformations, as in the Cyclic Extrusion and Compression (CEC) [12], or superimposing different strain fields, as in the Torsion Extrusion (TE). Other authors [13, 14] developed forging-like approaches such as the High-Pressure Torsion (HPT), the Multidirectional Forging (MDF) and the Cyclic Closed-Die Forging (CCDF) to obtain bulk components or applied to roll-processes such as the Equal Channel Angular Rolling (ECAR) to obtain sheets components. Regarding the

use of tubes in the SPD processes, some authors carried out attempts [15-17], starting from traditional processes like extrusion and compression, with setups similar to those used to produce bulk samples, or spinning, using incremental processes such as flowforming.

1.2. Use of Zn in the SPD processes

Compared to the extensive literature on the SPD processes applied to titanium or magnesium parts, only a few papers have been published on the processing of ultrafine-grained pure zinc parts due to the fact that their low strength and brittleness are considered not ideal for manufacturing load bearing implants.

Srinivasarao et al. [8], using the High Pressure Torsion process of pure zinc, carried out one of the first attempts, changing the number of turns and evaluating the variation of the in-plane tensile properties and the hardness. It was shown that microhardness remains constant up to equivalent strains of about 60 and slightly decreases at higher strains, while the measured yield strength rises as the number of anvil revolutions increases. By using the Equal Channel Angular Pressing, Bednarczyk et al. [9] investigated different low-alloyed binary zinc alloys, obtaining, in the case of pure zinc, a decrease of the grain size from 509 µm up to 19.5 µm, without significant increase in the yield stress or in the ultimate tensile stress.

2. Tube flowforming process

2.1. State of the art

Tube flowforming allows manufacturing cylindrical parts using machines that employ two or three rollers. In this process the blank is mounted on a rotating mandrel and, using the rollers can move along the axis and radially to reduce the tube wall thickness. Thus, the internal diameter of the component remains constant, while the external diameter decreases during the process, increasing the length of the workpiece. As the workpiece volume is constant, with negligible tangential flow, the final component length L_1 can be calculated, according to Wong et al. [17], as:

$$L_1 = L_0 \frac{t_0(d_{int}+t_0)}{t_1(d_{int}+t_1)} \quad (2)$$

where L_0 is the initial length, d_{int} is the internal diameter of the workpiece and t_0 and t_1 are the initial and the final tube thickness.

The direction of the material axial flow allows classifying two flowforming methods, namely forward and backward, represented in Fig. 2.

In the case of forward flowforming (the upper side of Fig. 2) the material flows in the same direction of the rollers displacement and the part that has not been worked is driven ahead of the rollers. The tube is held between the mandrel and the tailstock, which requires a base or a flange to allow it to clamp against the part.

Backward flowforming (see the lower side of Fig. 2), which is particularly suitable when the material ductility of the blank is too low to accommodate tensile stresses, is generally used for blanks without a base or inner flange [17]. The workpiece is pushed against the mandrel using the pressure generated by the displacement of the rollers and material flows under the rollers in the opposite direction of the displacement towards the unsupported end of the mandrel. The deformed material in the contact zone presents three-dimensional compressive stress state, which helps to improve the material formability and refine the microstructure, as reported by Xia et al. [18].

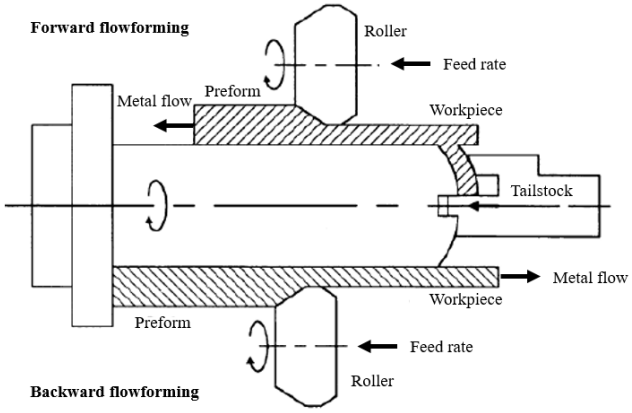

Fig. 2. Forward and backward flowforming process [17].

2.2. Experimental apparatus setup

The flowforming trials were performed on a Mori Seiki™ NL 1500 CNC lathe equipped with a backward tube flowforming apparatus, with a maximum value of axial force generated by the tailstock equal to 3000 N. Fig. 3a shows schematically the tube flowforming process while Fig. 3b shows the overall experimental equipment, fixed on the lathe.

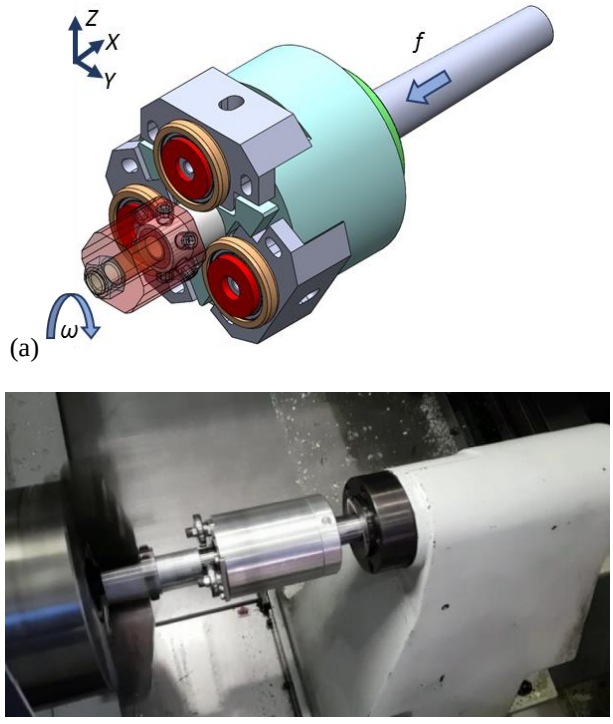

Fig. 3. Backward flowforming process: (a) scheme; (b) experimental setup.

According to the most modern machines, that employ a three-roller configuration to achieve a better balance of loads, three rollers are used, see Fig. 4. The rollers are spaced circumferentially at 120 deg, providing a uniform load distribution, and can be offset or staggered at a specific distance in the axial and radial direction, changing the reduction per pass and the strain imposed to the workpiece. The tube rotates along the X-axis at a constant angular velocity (ω), while the three rollers move at a constant feed rate (f) along the same axis.

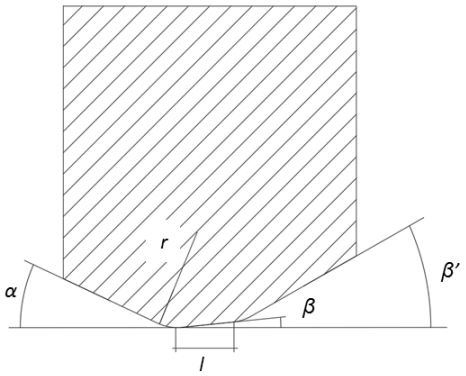

Fig. 4. Key dimensions of roller.

The double-tapered rollers, shown in Fig. 4, were designed to improve the surface smoothness of spun tubes. For thin-walled soft materials, such as aluminium or zinc alloys, the suitable forming angle α is 15-30°, sleeking angle β is usually 3-5°, receding angle β' is 20-30°, fillet radius r is 3-10 mm, and polishing belt length l is 3-6 mm, as reported by Xia et al. [10]. Therefore, the key geometric dimensions of rollers are set as reported in Table 1.

Table 1. Geometrical parameters of rollers.

Parameters	Values
Roller radius R (mm)	35
Forming angle α (°)	25
Sleeking angle β (°)	3
Receding angle β' (°)	30
Fillet radius r (mm)	3
Polishing belt length l (mm)	6

3. Experimental

3.1. Material

The material object of the investigation is zinc 99.99% provided in bar of 30 mm of diameter. The nominal chemical composition is reported in Table 2. A 60 mm length tube with an internal diameter of 25 mm and an external diameter equal to 30 mm was made using the bar.

Tensile and microhardness tests were carried out to characterize the material, in particular for the evaluation of the maximum elongation and the ultimate tensile strength, while to calibrate the material model for numerical simulations compression tests were performed. In addition, the microstructural characteristic of the initial bar was evaluated to investigate the grain size variation.

Table 2. Zinc 99.99% nominal chemical composition in wt. %.

Element	Wt. %
Zn	base
Pb	≤ 0.005
Cd	≤ 0.003
Fe	≤ 0.003
Sn	≤ 0.001
Cu	≤ 0.002

Six indentations, repeated three times, were carried out to evaluate the hardness of the as-delivered zinc, using a 98.1 mN load and 15 seconds dwell time. The indentations, spaced circumferentially at 60 deg apart as shown in Fig. 5, provide an average value of HV equal to 35.7 ± 2.5, while for each of the six indentations the uncertainty includes the maximum and minimum value of the three measurements.

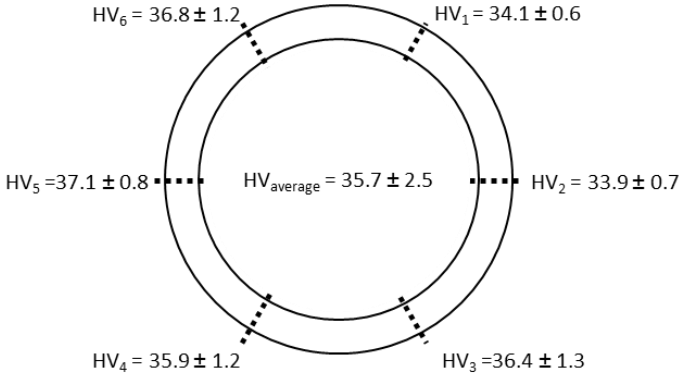

Fig. 5. Zinc 99.99% average values of HV.

The samples were cut and prepared for microstructural analysis using SiC papers for grinding and colloidal silica for final polishing. The grain structure was revealed by etching using a solution of 5 ml of HCl and 95 ml of H_2O. The microstructure was examined using a Leica DMRE™ Optical Microscope (OM). Fig. 6 shows the microstructure in the as-delivered condition, the initial grain size was measured by linear intercept method and resulted equal to 287 ± 72 µm. The high standard deviation value highlights the inhomogeneity of the initial microstructure.

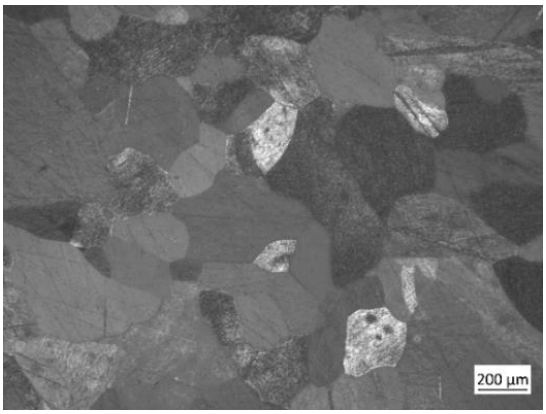

Fig. 6. Zinc microstructure in the as-delivered conditions.

Fig. 7 reports the engineering tensile curves at room temperature carried out at a strain rate of 1 s^{-1} using a 8 mm diameter round sample, cut from the zinc bar, showing a yield strength of 8 MPa. The main mechanical properties of the material in the as-delivered conditions, obtained from the tensile tests, are reported in Table 3.

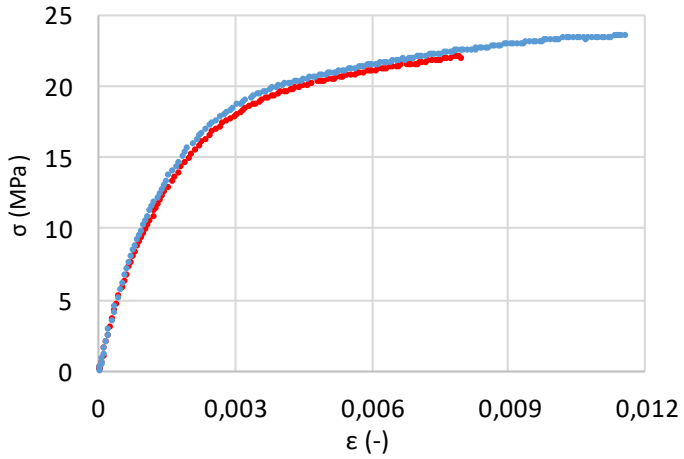

Fig. 7. Zinc stress-strain curves in the as-delivered conditions.

Table 3. Zinc 99.99% mechanical properties in the as-delivered condition.

Dimension	Value
UTS (MPA)	23.5±1.2
Max Elongation (%)	0.009±0.003

Fig. 8 shows the stress-strain curves of uniaxial compression tests carried out at a strain rate of 1 s^{-1} using a cylindrical specimen with a length of 14 mm and a diameter of 10 mm.

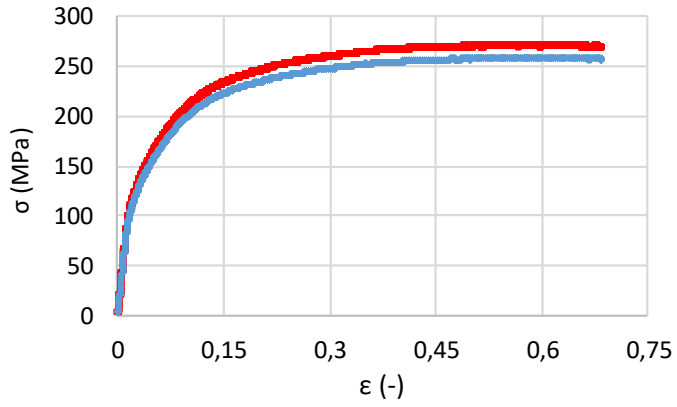

Fig. 8. Zinc stress-strain curve in the as-delivered conditions.

4. Numerical FE model

A finite element simulation of the backward tube flowforming was adopted to study the deformation characteristics and the axial displacement distribution. The simulation was developed using the software Forge NxT 3.0™ considering a 15 mm of rollers' stroke to reduce the time of calculation.

The influence of different process parameters was investigated, namely the rollers' reduction per pass, the mandrel speed, the feed rate on the forces and strains during the process, as reported in Table 4. Two mandrel speeds, equal to 300 rpm and 600 rpm, were considered, while for each of these rotational speeds three different feed rate are used. Concerning the reduction per pass, three different configurations were chosen, with a total reduction equal to 0.15 mm, 0.20 mm and 0.75 mm.

Table 4. Numerical simulations plan.

Number	Mandrel speed (rpm)	Feed rate (mm/s)	Reduction per pass (mm)		
			Roller1	Roller2	Roller3
1	300	1	0.05	0.10	0.15
2	300	1	0.05	0.15	0.20
3	300	1	0.10	0.40	0.75
4	300	1.5	0.05	0.10	0.15
5	300	1.5	0.05	0.15	0.20
6	300	1.5	0.10	0.40	0.75
7	300	2	0.05	0.10	0.15
8	300	2	0.05	0.15	0.20
9	600	1	0.05	0.10	0.15
10	600	1	0.05	0.15	0.20
11	600	1	0.10	0.40	0.75
12	600	1.5	0.05	0.10	0.15
13	600	1.5	0.05	0.15	0.20
14	600	1.5	0.10	0.40	0.75
15	600	2	0.05	0.10	0.15
16	600	2	0.05	0.15	0.20

4.1. Numerical model set-up

The model set-up is presented in Fig. 9a and Fig. 9b. The workpiece is considered elasto-plastic and it was modeled by mean of the Hooke equation for stress lower than *Y* and with the Hollomon equation for stress larger than *Y*, as reported in Eq. 3.

$$\sigma = \begin{cases} E\varepsilon & when\ \sigma < Y \\ K\varepsilon^n & when\ \sigma \geq Y \end{cases} \quad (3)$$

where *E* is the Young modulus, *K* is the strength coefficient the and *n* is the strain hardening coefficient.

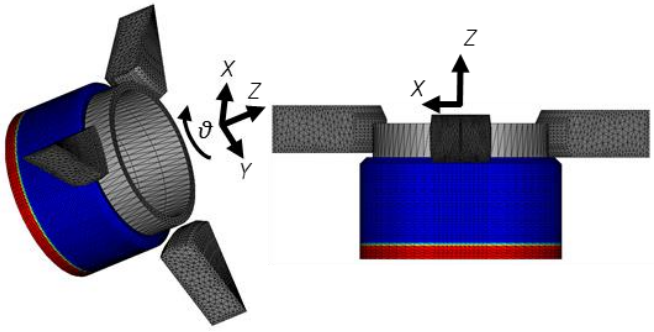

Fig. 9. Numerical FE model of backward flowforming: (a) perspective view; (b) lateral view.

The rollers and mandrel were modeled as rigid bodies. To simulate the effect of the tailstock and the tube rotation, the nodes at one end of the workpiece were constrained in Z and θ directions. The axial constraint aims at reproducing the mandrel that keeps the tube fixed, while the angular constraint was used to simplify the contact condition between the mandrel and the tube by imposing the spindle speed directly on the workpiece nodes.

4.2. Material model

The constitutive model of material implemented in the FE analysis was represented by the Hooke and Hollomon equations, as expressed in Eq. 3.

The numerical calibration of constitutive parameters was carried out through compression tests on a cylindrical specimen at room temperature. Table 5 reports the values of the constitutive parameters.

Table 5. Hollomon parameters.

Parameters	Values
K	359.015
n	0.26794

4.3. Numerical simulation results

Table 6 reports the results in terms of maximum elongation at the end of the rollers' stroke, the maximum total axial force to deform the tube and the maximum level of strain reached during the process. The former allowed to verify the process feasibility on the developed experimental setup, while the latter was used to identify the cross-section along the deformed tube for the microstructure and the microhardness evaluations.

From the simulation plan carried out it was possible to set the optimal process parameters, in particular the rollers' reduction per pass, the mandrel speed and the feed rate.

Table 6. Numerical simulations results.

Number	Elongation (mm)	Maximum force (N)	Maximum strain (-)
1	0.75	1079	1.185
2	0.99	1275	2.965
3	2.59	2836	5.814
4	0.80	1216	1.587
5	0.89	1301	4.407
6	1.56	2789	4.112
7	0.71	942	2.729
8	0.97	1373	3.237
9	0.85	1275	1.463
10	1.00	1343	3.201
11	2.43	2952	6.283
12	0.73	883	3.708
13	1.01	1472	3.479
14	2.63	2857	5.293
15	1.03	1766	4.889
16	0.71	1679	2.858

In the case of a total tube wall thickness reduction larger than 0.20 mm (as in the case of simulations 3, 6, 11 and 14), the buildup defect was generated, as shown in Fig. 10, independently on the feed rate value. For these reasons, the configurations 12 and 15 were chosen, with the characteristics summarized in Table 7 and Table 8.

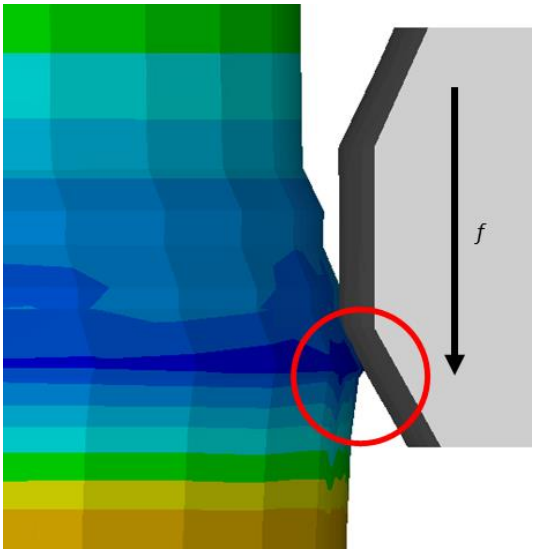

Fig. 10. Buildup defect for reduction per pass larger than 0.20 mm.

Table 7. Experimental plan for specimen 1.

Parameters	Values
Roller 1 reduction per pass (mm)	0.05
Roller 2 reduction per pass (mm)	0.10
Roller 3 reduction per pass (mm)	0.15
Number of pass (-)	1
Mandrel speed (rpm)	600
Feed rate (mm/s)	1.5
Rollers stroke (mm)	30

Table 8. Experimental plan for specimen 2.

Parameters	Values
Roller 1 reduction per pass (mm)	0.05
Roller 2 reduction per pass (mm)	0.10
Roller 3 reduction per pass (mm)	0.15
Number of pass (-)	1
Mandrel speed (rpm)	600
Feed rate (mm/s)	2
Rollers stroke (mm)	30

5. Results and discussion

According to the process parameters previously identified, two experimental tests were carried out, varying the feed rate from 1.5 mm/s for specimen 1 up to 2 mm/s for specimen 2 and using a constant mandrel speed equal to 600 rpm and a total reduction per pass equal to 0.15 mm. For the microhardness and microstructure experimental evaluations, two tube sections were considered (see Fig. 11a), while for each section three different radii were considered, the inner r_{int}, the middle r_{mid}

and the outer r_{ext}, to investigate the obtained grain refinement. In these sections, from the numerical simulation, the strain on the tube is respectively equal to 3.52 and 1.32 for configuration 1 and 4.74 and 1.54 for configuration 2.

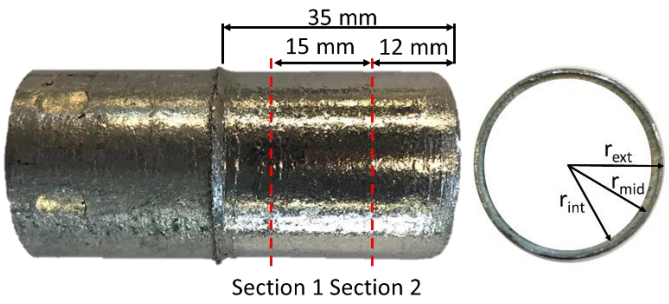

Fig. 11. Flowformed tube: a) cutting sections; b) sections.

5.1. Microhardness tests

Six indentations, repeated three times, were carried out varying the radius to evaluate the hardness of each section, using a 98.1 mN load and 15 seconds dwell time. The indentations, spaced circumferentially at 60 deg apart, provide the average values of HV reported in Table 8 for the specimen 1 and Table 9 for the specimen 2.

Table 8. Microhardness results for specimen 1.

Section 1	Values (HV)
Internal radius	43.4 ± 1.2
Middle radius	44.0 ± 0.8
External radius	54.5 ± 1.9
Section 2	Values (HV)
Internal radius	35.6 ± 1.1
Middle radius	46.5 ± 1.2
External radius	46.2 ± 1.7

Table 9. Microhardness results for specimen 2.

Section 1	Values (HV)
Internal radius	37.8 ± 0.9
Middle radius	38.6 ± 1.3
External radius	44.6 ± 1.5
Section 2	Values (HV)
Internal radius	34.6 ± 0.8
Middle radius	42.2 ± 1.5
External radius	43.2 ± 1.2

Fig. 12 reports the average value of HV as function of the tube radius. It was seen that in Section 1 the larger the radius the higher the microhardness for both the specimens, while Section 2 shows lower microhardness values, having lower values in the middle and outer radii. In addition, the microhardness is larger for specimen 1, processed with a feed rate equal to 1.5 mm/s.

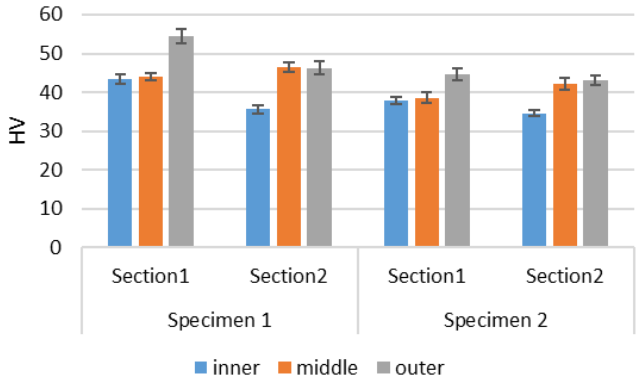

Fig. 12. Microhardness results for the two specimens.

5.2. Microstructures

Fig. 13 and Fig. 14 show the microstructure obtained respectively for specimen 1 and specimen 2. In both the cases it is possible to note a gradient of grain size moving from the inner to the outer tube radius. Comparing both the microstructures with the as-delivered zinc alloy, represented in Fig. 6, it was seen a relevant grain refinement with a homogeneous structure in the outermost portion of the tube.

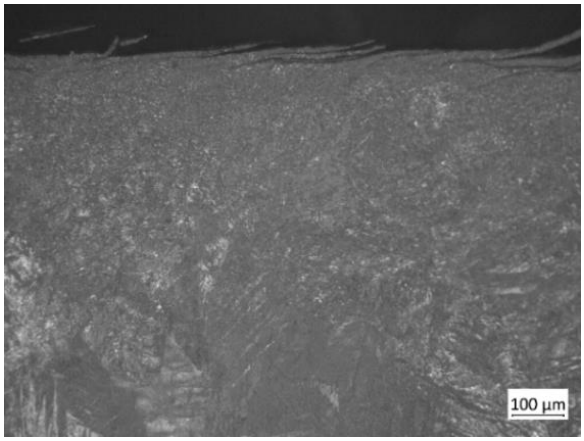

Fig. 13. Zinc microstructure in *specimen 1* process conditions.

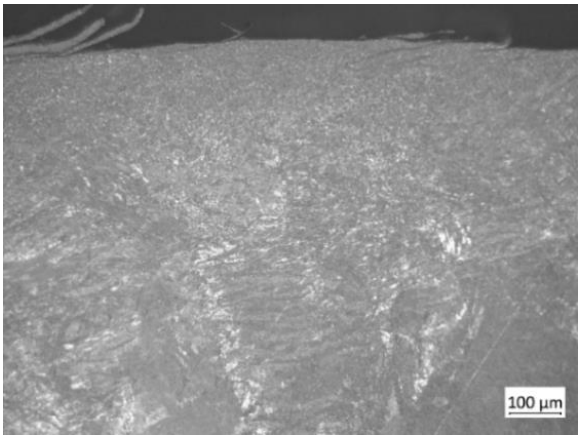

Fig. 14. Zinc microstructure in *specimen 2* process conditions.

6. Conclusions

The paper presents (i) the numerical results in terms of maximum forces and strain evolution during backward flowforming as function of the process parameters, and (ii) the experimental results in terms of microstructure and microhardness in case of two experimental configurations.

The numerical results show that:

- The axial force applied on the roller during the process is dependent on the reduction per pass and the mandrel speed and that it augments increasing the reduction per pass or decreasing the mandrel speed, while there is not a correlation with the feed rate.
- The strain during the process is dependent not only on the reduction per pass but also on the rollers' stroke and the mandrel speed, and the maximum value is obtained in the final part of tube that is deformed, due to the mechanism of deformation.

The experimental results show that:

- The microhardness varies over the radius and reaches maximum values at the outer diameter, while at the inner diameter values are similar to the microhardness on the as-delivered bar. The values have a homogeneous distribution, with similar microhardness at the same radius.
- The feed rate has an important role on the microhardness, with an increase on it decreasing the feed rate.
- The microstructures show that with the backward tube flowforming process it is possible to obtain a grain refinement in the external zone of the tube, with a decrease of the grain size from 287 µm up to 10 µm.

Acknowledgements

This research and development project was funded by "Severe plastic deformation by incremental processes - SPeDITO" ref. BIRD195839-2019.

References

[1] M. S. Dambatta et al., "Processing of Zn-3Mg alloy by equal channel angular pressing for biodegradable metal implants", *Journal of King Saud University*, 29, 455-461 (2017)

[2] R. Z. Valiev et al., "Bulk nanostructured materials from severe plastic deformation", *Progress in Materials Science*, 45, 103-89, (2000)

[3] M. Naito et al., *Evaluation Methods for Properties of Nanostructured Body*, Elsevier, Nanoparticle Technology Handbook (Third Edition), 301-363, (2018)

[4] M.A. Meyers et al., "Mechanical properties of nanocrystalline materials", *Progress in Materials Science*, 51, 427-556 (2006)

[5] G. Faraji at al., *Severe plastic deformation: methods, processing and properties*, Elsevier, (2018)

[6] Y. G. Jin et al., "Continuous high strength aluminium bolt manufacturing by the spring-loaded ECAP system", *Journal of Mater Processing Tech*, 212, 848-855, (2012)

[7] R. Z. Valiev et al., "Fundamentals of superior properties in bulk NanoSPD materials", *Mater Res Lett*, 4, 1-21 (2016)

[8] B. Srinivasarao et al., "On the relationship between the microstructure and the mechanical behavior of pure Zn processed by high pressure torsion", *Mat Sci & Eng*, 562, 196-202 (2013)

[9] W. Bednarczyk et al., "Can zinc alloys be strengthened by grain refinement? A critical evaluation of the processing of low-alloyed binary zinc alloys using ECAP", *Mat Sci & Eng*, 748, 357-366 (2019)

[10] A. Azushima et al., "Severe plastic deformation (SPD) processes for metals", *CIRP Annals*, 57, 716-735, (2008)

[11] R. Z. Valiev et al., "Principles of equal-channel angular pressing as a processing tool for grain refinement", *Progress in Meterials Science*, 51, 881-981 (2006)

[12] Q. Wu et al., "The microstructure and properties of cyclic extrusion compression treated Mg-Zn-Y-Nd alloy for vascular stent application", Journal of the Mech Behaviour of Biomedical Materials, 8, 1-7 (2012)

[13] A. Zhilyaev et al., "Using high-pressure torsion for metal processing: Fundamentals and applications", *Progress in Materials Science*, 53, 893-979, 2008

[14] I. Ansarian et al., "Microstructure evolution and mechanical behaviour of severly deformed pure titanium through multi directional forging", *Journal of Alloys and Compounds*, 776, 83-95 (2019)

[15] G. Faraji et al., "Tubular channel angular pressing (TCAP) as a novel severe plastic deformation method for cylindrical tubes", *Journal of Mater Lett*, 65, 3009-3012 (2011)

[16] G. Faraji et al., "Review of principles and methods of severe plastic deformation for producing ultrafine-grained tubes", *Journal of Mater Sci and Tech*, 33, 905-923 (2017)

[17] C.C. Wong et al., "A review of spinning, shear forming and flow forming processes", *Int Journal of Machine Tools & Manufacture*, 43, 1419-1435 (2003)

[18] Q. Xia et al., "A study of manufacturing tubes with nano/ultrafine grain structures by stagger spinning", *Mater & Design*, 59, 516-523, (2014)